17th World Conference on Earthquake Engineering, 17WCEE
Sendai, Japan - September 13th to 18th 2020

INFLUENCE OF COLUMN BASE FIXITY ON THE SEISMIC RESPONSE OF SINGLE STOREY BRACED FRAMES

J. Woods[1], R. Tremblay[2], N. Bouaanani[3]

[1] *Assistant Professor, Queen's University, joshua.woods@queensu.ca*
[2] *Professor, Polytechnique Montreal, robert.tremblay@polymtl.ca*
[3] *Professor, Polytechnique Montreal, najib.bouaanani@polymtl.ca*

Abstract

Gravity columns with exposed base plate connections are often assumed as pinned in both analysis and design. However, past experiments have shown that base plate connections can provide a significant level of flexural strength and stiffness depending on the depth of anchor rod embedment and the level of axial load carried by the gravity column. The goal of this study is to investigate the influence, if any, that the effect of base plate flexural strength and stiffness have on the global seismic response of single storey braced frames with flexible roof diaphragms.

To capture the nonlinear response of exposed base plate connections, a simplified approach to model exposed base plate connections suitable for nonlinear time-history analysis is developed in OpenSees. The OpenSees model uses compression-only elements to model the contact between the base plate and grout, nonlinear fiber elements to capture the flexural response of the steel base plate and tension-only elements to model the nonlinear response of the anchor rods. To validate the proposed modeling approach it is compared with available experimental data in the literature and detailed finite element models developed in Abaqus. The results show that the OpenSees model can capture the nonlinear cyclic response of exposed column base connections and is suitable for conducting nonlinear time-history analysis.

To investigate the influence of column base fixity on the system-level response of single-storey braced frames, the nonlinear dynamic response of two prototype single-storey steel concentrically braced frames with flexible roof diaphragms are investigated. The structures are designed for a site in Vancouver, British Columbia Canada and have different storey heights and footprints to investigate the influence that building geometry has on their response. Finite element models of each prototype structure are developed in OpenSees. The lateral load resisting system for the prototype structures is a tension-only braced frame system. The OpenSees model includes inelastic buckling of the tension-only X braces. The flexible steel deck roof diaphragm is modeled using shell elements in OpenSees. The developed models are subjected to a suite of 15 ground motion records representative of the regional seismicity in Western Canada.

Each prototype structure is subjected to the series of earthquakes with three different assumptions for the degree of base fixity: (1) pinned, (2) fixed and (3) a realistic base plate connection. The simplified base plate model developed in OpenSees is shown to be able to accurately capture the strength and stiffness of exposed base plate connections and is suitable for nonlinear time-history analysis. The results of the study show that the degree of column base fixity does not have a significant influence on the maximum displacement response of single storey steel braced frames with flexible roof diaphragms.

Keywords: base plate, steel, single-storey building, flexible diaphragm, nonlinear numerical models, finite elements

1. Introduction and Literature Review

Column base plate connections are used in virtually all types of steel structures to transfer forces and/or moments from the superstructure to their foundations. At the base of gravity columns, these connections are often assumed to be pinned in analysis and design, and thus do not contribute to the lateral load resistance of a structure. However, past experimental studies have demonstrated that steel column base plate connections can provide a significant level of flexural strength and stiffness at the base of a column depending on the thickness of the base plate, size and embedment depth of the anchor rods, and the level of axial load carried by the column. Figure 1 shows the typical components in an exposed base plate connection, which include the steel column, base plate, anchor rods and grout layer. Under lateral load, base plate connections can fail in a variety of modes depending on the thickness of the base plate and size of the anchor rods, shown in Fig. 1. For thick base plates, failure will initiate through yielding of the anchor rods in tension. For thin base plates, failure is initiated through yielding of the base plate in bending, which can occur on both the compression and tension side of the plate. Under the presence of axial load, exposed base plate connections will exhibit a self-centering hysteretic response behaviour, in which the energy dissipation results from yielding of the anchor rods in tension, bending of the steel base plate, or both and the self-centering behaviour results from the presence of the gravity load. The goal of this study is to investigate the influence, if any, that the effect of this behaviour has on the global seismic response of single storey braced frames with flexible roof diaphragms.

Several studies have focused on investigating the behaviour of exposed steel base plate connections in steel structures. Experimental studies by [1-3] investigated the strength and behaviour of typical base plate connections under axial load and lateral displacement. Experimental results are complemented by analytical studies and the development of design approaches [4-5], all of which have contributed to the modern design methods for column base plate connections [6]. More recent studies have been carried out to validate the proposed design approaches and investigate the influence of base plate thickness, anchor rod size, and axial load on the lateral strength and stiffness of exposed base plate connections [7-9]. Although these studies have shed light on the behaviour of column base plate connections, most of the focus in these works is on base plate connections in moment frames, while comparatively less research has focused on the contribution of base plate rigidity in braced frame buildings, particularly their influence on system-level seismic response.

To address this gap and examine the influence that assumptions about the degree of column base fixity have on the seismic response of steel braced frame structures, a simple numerical model for base plate connections has been developed in OpenSees. The performance of the OpenSees model is validated against experimental results and detailed finite element models developed in ABAQUS. The results show that the OpenSees model can capture the nonlinear hysteretic response behaviour of exposed column base connections with reasonable accuracy, including their ultimate strength, ductility, and self-centering response. The simple nature of the developed model makes it suitable for conducting nonlinear time-history analysis.

Based on promising results from the simplified OpenSees model, it is employed to model the base plate connections in a full-scale building model and examine the influence of column base fixity on the syste-level seismic response of two single-storey braced frames with flexible roof diaphragms. The two prototype structures have different sizes and storey heights to investigate the influence that building geometry has on their response.

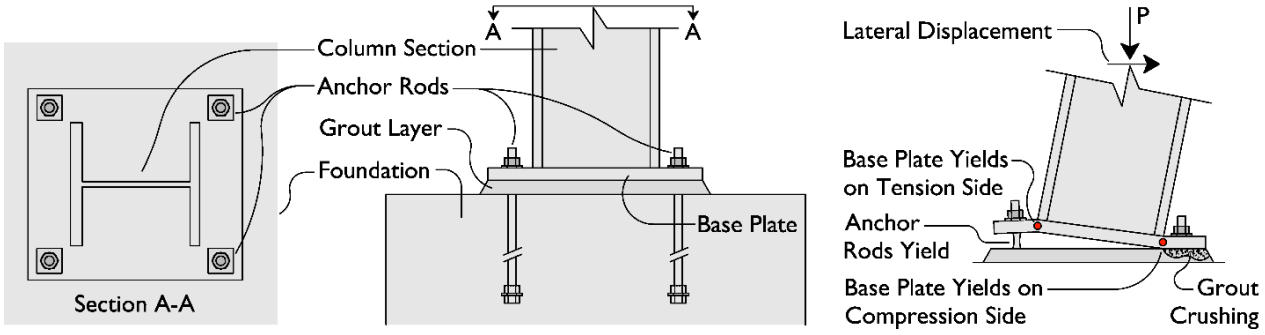

Fig. 1 – Typical steel gravity column base plate connection and failure modes

2. Numerical Modeling

Prior to evaluating the influence of column base fixity on the global seismic response of single storey braced frames, two different finite element models were developed: (1) a detailed three-dimensional model used to validate experimental results, and (2) a simplified two-dimensional model suitable for nonlinear time-history analysis. The experimental data used to validate the developed models is from a study by Gomez et al. (2010) [7]. Figure 2 shows the design details for one of the base plate connections tested by [7]. The W200×71 column had a 355×355 mm steel base plate, 25.4 mm thick, with 4 - 19 mm anchor rods embedded 520 mm into a concrete foundation. The base plate was fabricated of ASTM A36 steel, while the anchor rods were ASTM F1554 Grade 105, with the material properties listed in Fig. 2. Although other base plate designs were tested by [6] (e.g. different plate thickness and number of anchor rods), the tested base plate connection that were most representative of a gravity column base plate connection were selected for comparison in this study. In the study by [6], two identical base plate connections were tested with and without axial load under a predefined reversed cyclic load sequence. Each connection was subjected to the SAC reversed cyclic loading protocol, which is intended to represent deformation histories that are consistent with seismic demand in special moment frame buildings [10]. For each experiment, the load sequence consisted of 6 cycles at 0.25%, 0.5%, and 0.75% drift, 4 cycles at 1% drift, and 2 cycles at 1.75%, 2%, 3%, 4%, and 5% drift.

3.1 Three-dimensional Finite Element Modeling

A detailed three-dimensional (3D) Finite Element (FE) model of the base plate tested by [7] was built in ABAQUS [11]. The concrete foundation, grout layer, steel base plate, anchor rods, and steel column were all modeled using solid 8-node brick elements with reduced integration (C38DR). Figure 2b shows the components of the model and the mesh. Four surface-surface interactions were used to define contacts in the model: (1) between the anchor rods and concrete foundation, (2) between anchor rods and grout, (3) between the steel base plate and grout, and (4) between the steel washers and the base plate. For the steel-concrete and steel-grout interactions, the normal behaviour was defined as 'hard contact', while a penalty friction model with a coefficient of friction of 0.45 was assigned in the tangential direction, according to recommendations by [10]. For the steel-steel interaction, the normal behaviour was also defined as 'hard contact', while a penalty friction model with a coefficient of friction of 0.8 was assigned in the tangential direction [10]. A higher mesh density was used for the anchor rods and base plate to accurately determine their local behaviour and any regions of high stress concentrations. A higher mesh density was also used between the base plate and grout to improve convergence rates for the contact interaction.

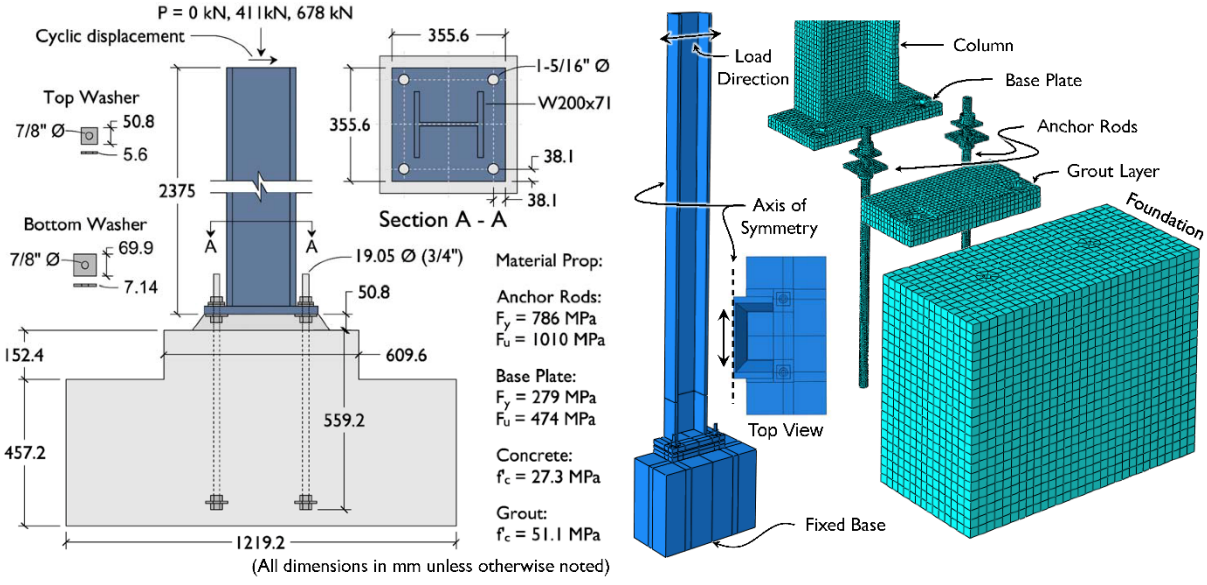

(a) (b)

Fig. 2 – (a) Base plate connection tested by Gomez et al. (2010); (b) Detailed finite element model

The plasticity material model with isotropic hardening was used to model the nonlinearity in the base plate and steel anchor rods. Material properties for the anchor rods and base plate were assigned the true-stress and plastic strain values from coupon tests conducted by [7], which are shown in Fig. 2. The steel column in the experiments remained elastic, and therefore was modeled using elastic material properties and a modulus of elasticity of 200 GPa. Observations during the tests also indicated that the concrete foundation was not damaged and remained elastic. Thus, the concrete foundation was modeled using an elastic material with a modulus of elasticity of 30 GPa based on the tested material properties of the concrete. The grout was modeled using the damage plasticity model in ABAQUS. The constitutive model for the concrete in compression, first proposed by Popovics [12], was used to account for inelasticity in the response of the grout. In this model, the relationship between the compressive stress (f_c) and compressive strain (ϵ_c) in the grout is given by:

$$\frac{f_c}{f_c'} = \frac{n(\epsilon_c/\epsilon_{co})}{(n-1)+(\epsilon_c/\epsilon_{co})^n} \tag{1}$$

where f_c' and ϵ_{co} are the compressive strength and strain corresponding to the maximum stress, respectively, and n is computed as $0.4\text{x}10^{-3}f_c'(\text{psi})+1.0$. In tension, the relationship between the tensile stress (σ) and tensile strain (ϵ_t) in the grout is given by:

$$\sigma = f_t(\epsilon_t/\epsilon)^{(0.7+1000\epsilon)} \tag{2}$$

where f_t is the cracking stress of the concrete and ϵ_t is the strain at cracking. The parameters for the concrete damage plasticity model included a dilation angle of 31 degrees, a flow potential eccentricity of 0.1, a K_c value of 0.667, and a viscosity parameter of 0.001. The viscosity parameter improves convergence during softening while maintaining accurate results, the appropriate value for which was determined using a sensitivity analysis.

Figure 3 shows the hysteretic force-deformation response of the two base plate connections tested by [7] and the results from the detailed finite element model in ABAQUS. The results show that the ABAQUS model accurately captures the inelastic cyclic response of the base plate connection with and without axial load. The model does a good job at predicting the initial stiffness, ultimate strength, post-yield stiffness and energy dissipation capacity of the connections. Without axial load, the connection exhibits a highly pinched hysteretic response because of permanent elongation of the steel anchor rods under lateral load. Once the anchor rods are permanently deformed, the base plate can undergo lateral displacement freely until the base plate makes contact with base of the anchor rods and they re-engage in tension. With the addition of axial load (Fig. 3b), the response of the base plate connection is similar but exhibits a flag-shaped self-centering response because of the restoring force provided by the gravity load. Energy dissipation at small lateral displacements is due to yielding of the base plate in tension and compression. Note that thick base plates will not yield and the connection will exhibit a more classical flag-shaped hysteretic rocking response behaviour.

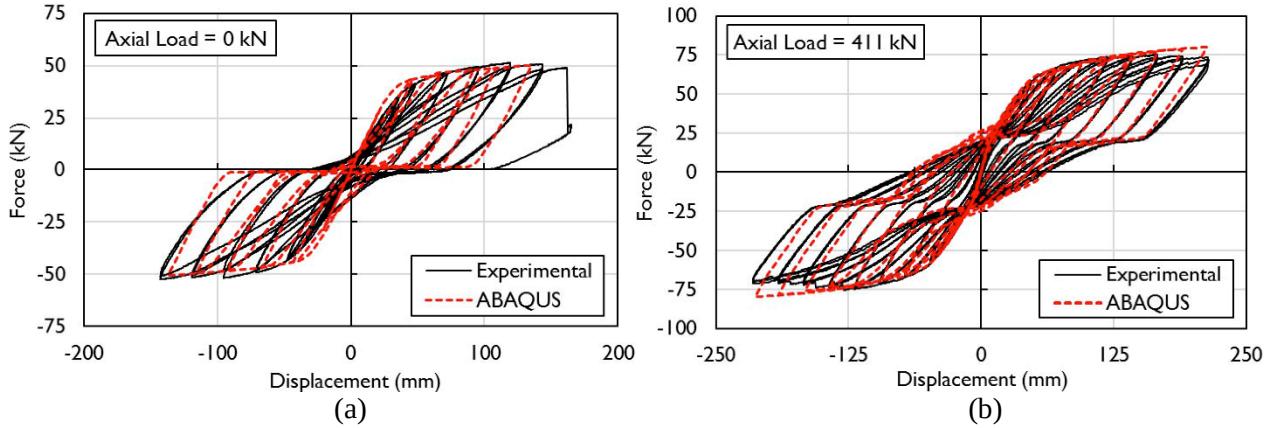

Fig. 3 – Hysteretic response behaviour of detailed base plate connection model in ABAQUS: (a) no axial load; (b) axial load of 411.5 kN (Experimental data from [7])

3.2 Fiber Element Modeling

While the developed 3D FE model satisfactorily predicts the inelastic cyclic response of the studied base plate connection, it is not suitable for system-level time-history analysis because of the large number of elements and contact surfaces in the model, which translates into long analysis times. To overcome this challenge and study the influence of column base fixity on the system-level seismic response of steel braced frame structures, a simple base plate connection model suitable for time-history analysis is developed in the fiber element software OpenSees [13]. Figure 4 illustrates the two-dimensional model developed in this study to investigate the hysteretic response of the base plate connections tested by [7]. The column is modeled using an elastic beam column element because no yielding was observed in the column during experimental testing by [7]. The portion of the base plate being restrained between the flanges of the steel column, assumed to be equal to 95% of the column depth *(d)* is also modeled using elastic beam-column elements. To model the inelastic response of the base plate, nonlinear beam-column elements are employed for the portion of the base plate outside of the flanges (outside of 0.95*d*),. The nonlinear elements are assigned a fiber section with the width *(d)* and thickness *(t)* of the base plate. The *Steel02* nonlinear uniaxial material model in OpenSees is assigned to the steel fibers, which includes isotropic strain hardening and the Bauschinger effect.

Under cyclic loading, the base plate lifts off of the grout layer, inducing tension in the anchor rods and causing them to extend. If the displacement is large enough, the anchor rods will yield and undergo permanent deformation. During load reversal, the base plate makes contact once again with the grout layer and the anchor rods on the opposite side of the base plate will be in tension. To capture this behaviour in the simplified OpenSees model, the steel anchor rods are modeled using two-node link elements, which are assigned a tension-only bi-linear force-deformation relationship using the *ElasticPPGap* uniaxial material model. Figure 4 illustrates the cyclic response of the material model assigned to the two-node link elements. The initial stiffness of the anchor rods (k_{anchor}) in the force-deformation relationship is determined using:

$$k_{anchor} = E_S \, A_{anchor} \, / L_{anchor} \tag{3}$$

where E_s is the modulus of elasticity of the anchor rod material, A_{anchor} is the area of the anchor rod and L_{anchor} is the embedment length of the anchor rod in the concrete foundation. In this study, the anchor rod have a modulus of elasticity of 230 GPa, an area of 285 mm^2 and a length of 560 mm. The anchor behaves elastically up to the yield force (P_y), determined based on the yield stress of the anchor rod material ($P_{y,anchor}=A_{anchor} F_y$). Note that two two-node link elements are used to represent the four anchor rods in the base plate connection by defining two times the area in Eq. 3. The damage option is used in the material definition to specify that damage will accumulate in the material, meaning that a gap beneath the anchor will be permitted to form. To capture fracture of the anchor rods in tension, the *MinMax* material model is used to set a limit on the maximum displacement of the anchor rods. The maximum elongation of the anchor rods was 16.5 mm, which correlated well with experimental results. After reaching the maximum elongation, the anchor rods are assumed to have failed and zeroes are then assigned for the element force and stiffness.

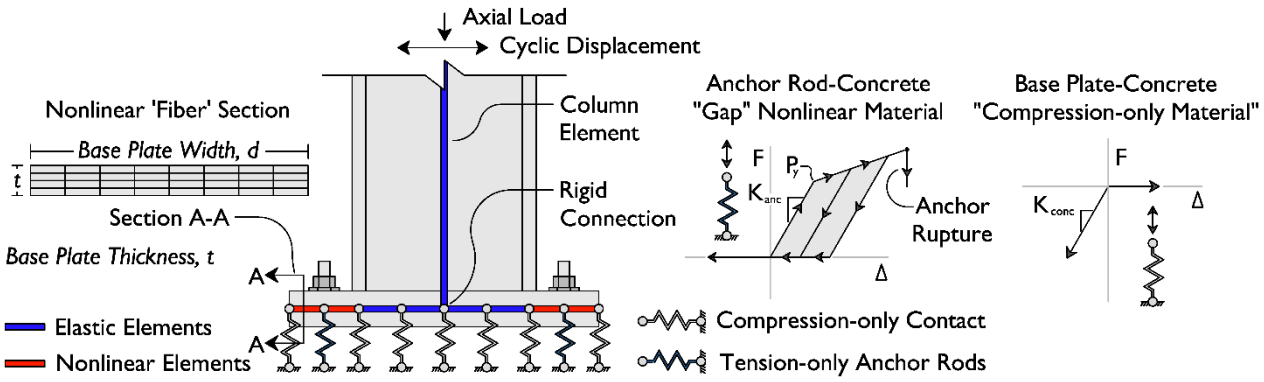

Fig. 4 – Simplified exposed base plate connection model in OpenSees

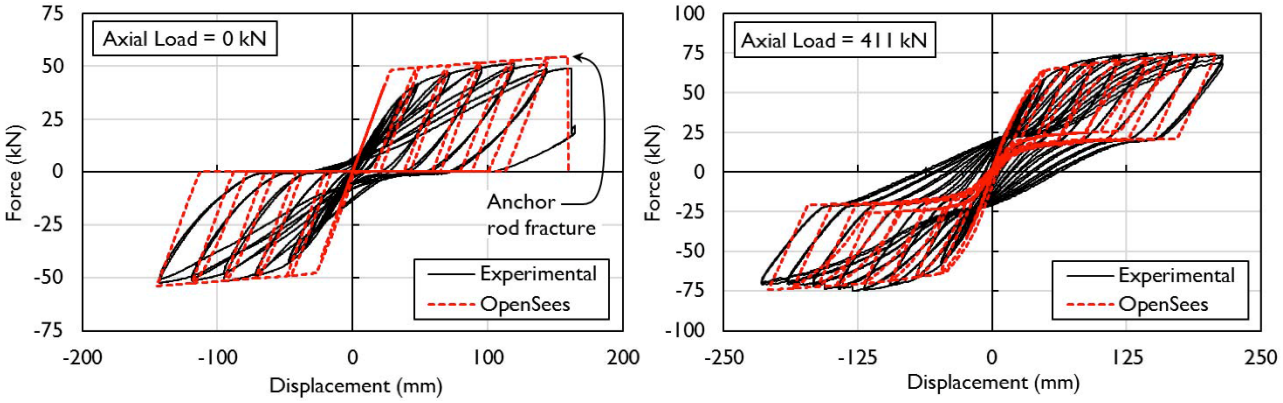

Fig. 5 – Hysteretic response behaviour of simplified base plate connection model in OpenSees: (a) no axial load; (b) axial load of 411.5kN (Experimental data from [7])

To model the interaction between the bottom of the base plate and grout layer, a series of two node link elements were used to simulate contact along the length of the base plate, as shown in Fig. 4. Under cyclic load, the base plate is free to uplift from the foundation, assuming there is no cohesion between the bottom of the base plate and concrete footing. To capture this behaviour, each of the two-node links was assigned a compression-only force-deformation relationship using the *ElasticPPGap* model. In the positive (upward) direction, the two-node links have zero stiffness, while in the negative (downward) direction, they have an elastic stiffness equal to the compressive stiffness of the concrete ($k_{concrete}$), determined using:

$$k_{concrete} = E_c \, A_{bp} \, / d_{footing} \tag{4}$$

where E_c is the modulus of elasticity of the concrete, taken as 30 GPa, A_{bp} is the plan area of the steel base plate, and $d_{footing}$ is the depth of the concrete footing. The resulting stiffness was divided evenly along the bottom of the base plate, resulting in a compression-only spring stiffness of approximately 400 kN/mm for each spring. It is noted that the stiffness of the compression-only concrete springs does not have a significant influence on the hysteretic response behaviour of the base plate connections studied in this paper. In this study, the nonlinear response of the grout in the simplified OpenSees model is ignored.

Figure 5 compares the results of the simplified base plate connection model in OpenSees with the experimental results from [7]. Without axial load, the results show that the model predicts well the cyclic response of the base plate connection, including accurately capturing its ultimate strength, post-yield stiffness and anchor rod fracture using the *MinMax* material model. With the presence of axial load, the model still satisfactorily predicts the ultimate strength and post-yield stiffness of the connection, but does not completely capture the energy dissipation capacity observed in the hysteretic force-deformation relationship. Some of the reasons for the observed discrepancies between the analytical and experimental response include ignoring the inelastic response of the grout and 3D effects (i.e. base plate bending out of plane) not captured in the simplified two-dimensional mode. Nonetheless, the simplified model reasonably predicts the nonlinear cyclic response of the base plate connection and is employed to analyze the influence that column base fixity has on the system-level seismic response of steel braced frame buildings.

4. Analysis of Single-Storey Structures

4.1 Prototype Single Storey Buildings

Based on satisfactory performance of the two-dimensional base plate connection model in OpenSees, it is used to study the influence of column base fixity on the seismic response of single storey concentrically braced frames with flexible roof diaphragms. The study was limited to single-storey structures rectangular in plan and included two building sizes of 30.4×30.4 m and 76×45.6 m with storey heights of 6.6 m and 8.6 m, respectively, which are representative of single-storey industrial buildings. For both buildings, the roof dead

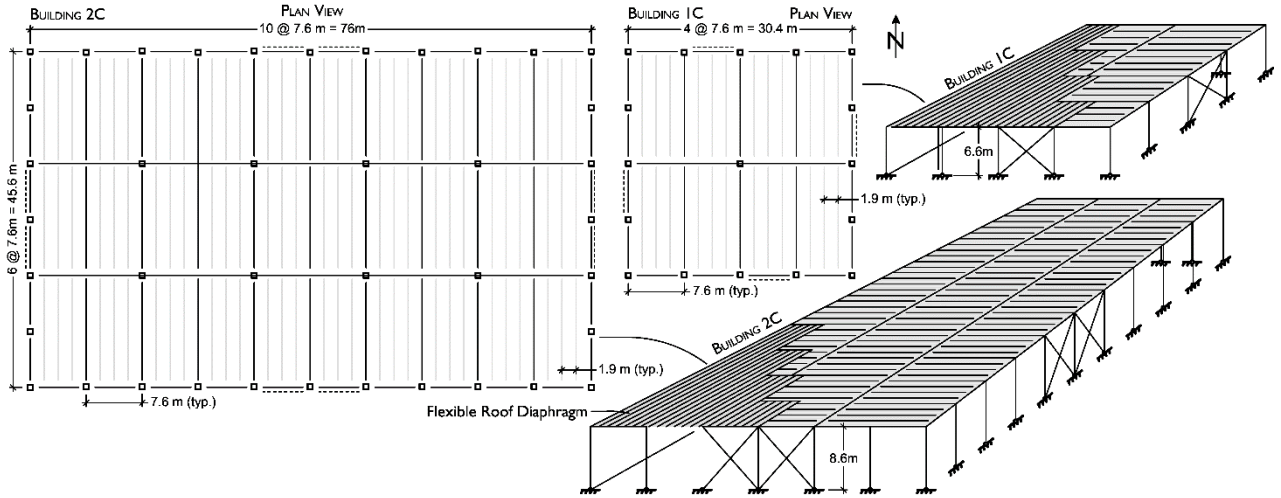

Fig. 6 – Prototype single-storey building with flexible roof diaphragm

and snow loads are assumed to be 1.2 kPa and 1.64 kPa, respectively. The walls of the building are fabricated of light-weight steel cladding, assumed to have a weight of 0.5 kPa. Figure 6 shows the two prototype buildings that are analyzed in this study and Table 1 shows the structural members for each building. The gravity load resisting system in each building is comprised of a steel deck diaphragm, open-web steel joists, W-shaped simply supported beams, and HSS-shaped exterior columns, which are reflective of typical construction practices for these industrial buildings in Canada. The steel deck had yield and ultimate strengths of 230 MPa and 310 MPa, respectively. The open-web steel joists were spaced at 1.9 m on center for both buildings.

The structures are designed according to the National Building Code of Canada [14] and the Canadian Design Standard for Steel Structures (CSA S16) [15] for a site in Vancouver, British Columbia Canada. The SFRS in each prototype building is a tension-only concentrically braced frame (X-configuration), which has ductility and over-strength factors (R_d and R_o) of 3.0 and 1.3, respectively. The braces are ASTM A500 grade C HSS sections, with yield and ultimate strengths of 345 MPa and 460 MPa, respectively. Table 2 shows the design details (e.g. thickness, fastener pattern and spacing) for the steel deck of each prototype structure, the design of which was based on gravity and lateral load requirements, including determining the expected shear in the diaphragm based on the strength of the bracing members in tension and compression.

Finally, because the primary objective of this study was to investigate the influence of column base fixity on the seismic response of single storey braced frames, base plates were designed for the columns throughout the structures. The procedure outlined in CSA S16 [15] was used to design the base plates, which are similar to the design procedure outlines in the ASCE Design Guide One [6]. These procedures assume a uniform allowable bearing pressure *(f_b)* beneath the base plate, computed using:

$$f_b = 0.85 f_c' A_1 \sqrt{A_1/A_2} \leq 1.7 f_c' A_1 \tag{5}$$

where A_1 is the bearing area under the column and A_2 is the projected bearing area underneath the column determined by extending the bearing area outwards at a 45 degree angle until reaching the base of the foundation footing. Based on the allowable bearing pressure in the concrete, the required dimensions of the base plate can be determined and the required thickness of the base plate *(t_p)* can be evaluated using:

$$t_p = \sqrt{2 P_f l^2 / BC\phi F_y} \tag{6}$$

where P_f is the design axial load, l is the minimum of n or m, B and C are the dimensions of the base plate in plan and ϕF_y is the allowable stress in the steel base plate. Note that the lightly loaded base plate condition is not checked in this study because HSS sections are used for the columns throughout the structure, which do not exhibit this phenomenon. All of the base plate designs include 4 - 19.05 mm (3/4 in.) steel anchor rods according to the recommendations of CSA S16, even for columns that only support gravity load, to ensure

Table 1 – Prototype building design geometry and sections

Building	Dimensions ($l \times w$)	Beams (N-S)	Beams (E-W)	Exterior Column	Interior Column	Braces
1C	30.4×30.4m	W200×22	W310×45	HSS178×6.4	HSS178×7.9	HSS76×3.2
2C	76.0×45.6m	W250×39	W310×60	HSS203×7.9	HSS178×7.9	HSS76×4.8

Table 2 – Flexible roof diaphragm and modal properties for prototype buildings

Building	Steel Deck Thickness (mm)	Fastener Pattern	Fastener Spacing (mm)	Base Shear (V) (kN)	G'	$t_{theoretical}$ (Eq. 7) (s)	$t_{analysis}$ (s)
1C	0.76	4/7	127	285	4.8	0.35	0.42
2C	0.76	9/7	112	700	18.6	0.61	0.54

Note: $\Delta_{theoretical}$ is based on Eq. 7 and $\Delta_{analysis}$ is based on the 3D OpenSees model of the structure;

stability during erection. The anchor rods had a design embedment of 310 mm (12 in.), which is a commonly encountered embedment depth in practice. The base plate design for a typical gravity column in both structures measured 400×400 mm and had a thickness of 25.4 mm.

4.2 Numerical Models

The numerical models of the prototype buildings in this investigation were constructed in OpenSees. Each building was subjected to a series of earthquake ground motion records. Three different sets of boundary conditions were considered: (1) pinned column bases, (2) fixed column bases and (3) realistic column bases using the 2D OpenSees base plate model. Figure 7 shows a typical building model for the prototype structures in this study. The structural response was studied in the N-S direction. The columns were modeled using elastic beam column elements. For the braces, each half brace was modeled using 10 nonlinear beam-column elements with fiber sections. The cross-section of the fiber element was assigned 8 fibers along its length and 4 fibers across its width, in addition to fibers assigned radially to model the corners of the HSS section (shown in Fig. 7). The *Steel02* material model was used to model material inelasticity and an initial imperfection equal to 1/500 of the braces length was introduced to initiate buckling behaviour. As shown in Fig. 7, one brace is modeled as a continuous element and the other brace is modeled as a discontinuous element with zero-length rotational springs used to model the rotational stiffness of the plate in the center of the brace. The gusset plates at the ends of the braces were modeled using elastic elements, with zero-length rotational springs at their ends to model the rotational stiffness of the gusset plate about each of its three principal axes.

To model the flexible roof diaphragm, three-dimensional (3D) shell elements were employed. The *ShellMITC4* 3D element object in OpenSees uses a bilinear isoparametric formulation in combination with a modified shear interpolation to improve thin-plate bending performance. Properties were assigned to the shell element using the *nDMaterial* command in OpenSees and the *ElasticOrthotropic* material model, which are assigned to a *PlateFiber* section to incorporate the element thickness, which is assumed to be equal to the thickness of the steel deck (shown in Table 2). In the elastic orthotropic material model for the diaphragm, a modulus of elasticity E=200GPa, a Poisson's ratios v=0.3, and a modified shear stiffness (G) were assigned to the shell elements to account for diaphragm flexibility. Finally, the fundamental period of the numerical models is compared with the recommended design period of vibration for steel braced frames with steel deck flexible roof diaphragms (T_a), which can be computed according to:

$$T_a = 0.035h_n + 0.004L \tag{7}$$

where h_n is the height of the building in meters and L is the length of the diaphragm, in meters, between adjacent vertical elements of the SFRS in the direction perpendicular to the direction under consideration. The period of vibration calculated using Eq. 7 may be increased by up to 1.5 times for buildings that are shown to have a higher predicted fundamental period of vibration using a structural model. Table 2 shows the properties of the flexible roof diaphragms and the fundamental period of vibration for each prototype structure based on the NBCC and from the OpenSees models. As expected, the results show that the period of vibration from the OpenSees models ($T_{analysis}$) are close to the predicted results using Eq. 7.

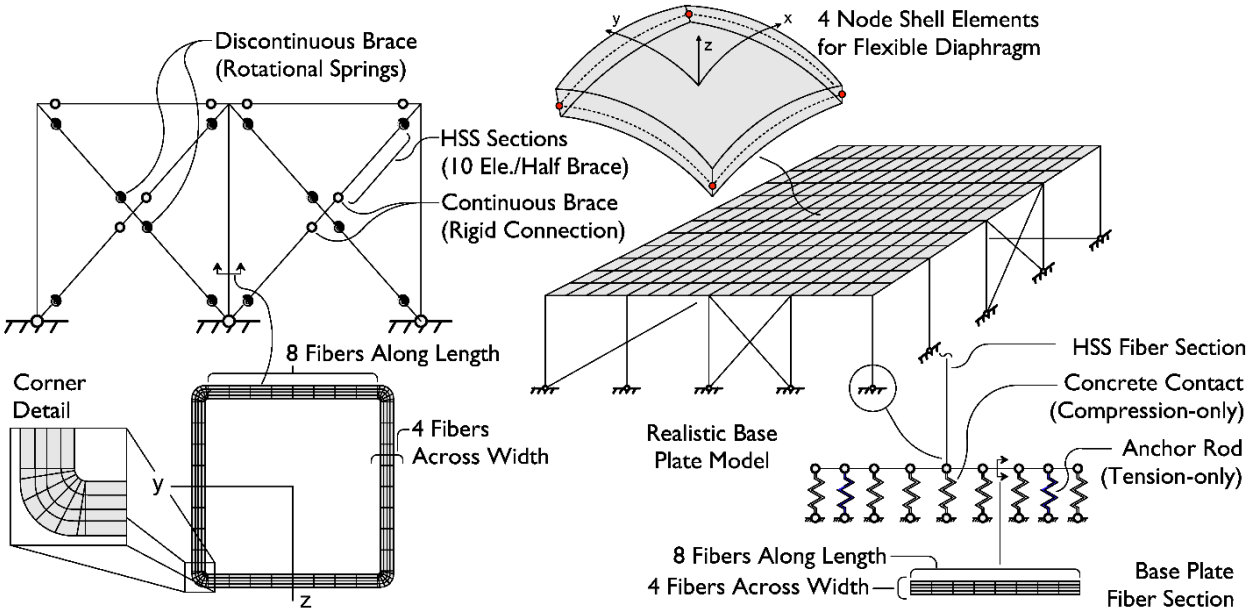

Fig. 7 – Numerical model of a typical prototype building in OpenSees

4.3 Earthquake Records

The two prototype structures were subjected to a suite of 15 earthquake ground motions scaled according to the procedures outlined in the NBCC (2015) [14] for site class C and the building design site in Vancouver, British Columbia, Canada. The design site is exposed to earthquakes from three seismic sources: (1) intraplate crustal earthquakes, (2) deep in-slab earthquakes and (3) subduction inter-plate earthquakes to ensure appropriate representation of each site source that contributes to the hazard in Vancouver. Figure 8 shows the acceleration response spectra for the 15 ground motion records (5 for each seismic source). The ground motion records from each seismic source were divided into three scenario-specific period ranges (T_R): (1) 0.3-1.0s for crustal earthquakes, 0.15-0.5s for subduction in-slab earthquakes and from 1.0s to the upper end of T_R for the subduction interface earthquakes. The records are scaled such that the mean spectrum of the subset does not fall more than 10% below the target spectrum at any period over the period range.

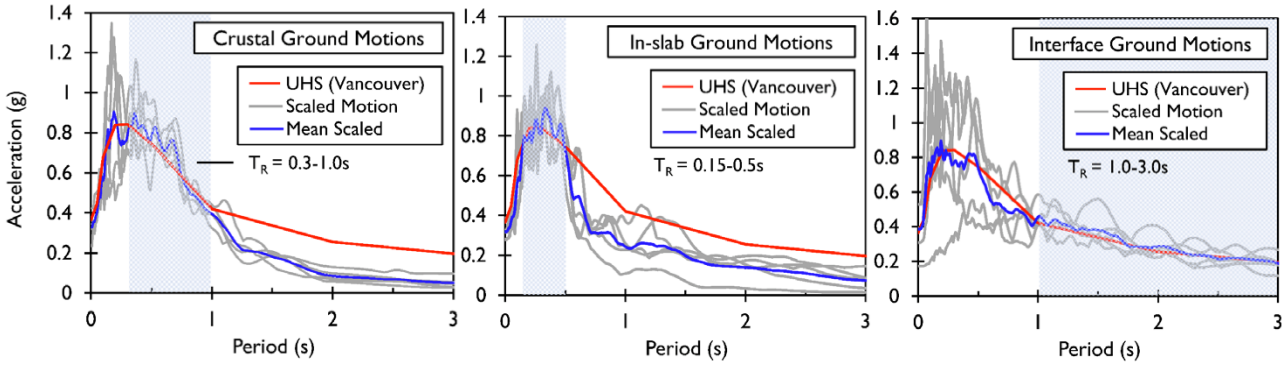

Fig. 8 – Three sets of 5 earthquake ground motions for nonlinear time-history analysis: (a) crustal ground motions; (b) in-slab ground motions; (c) interface subduction ground motions

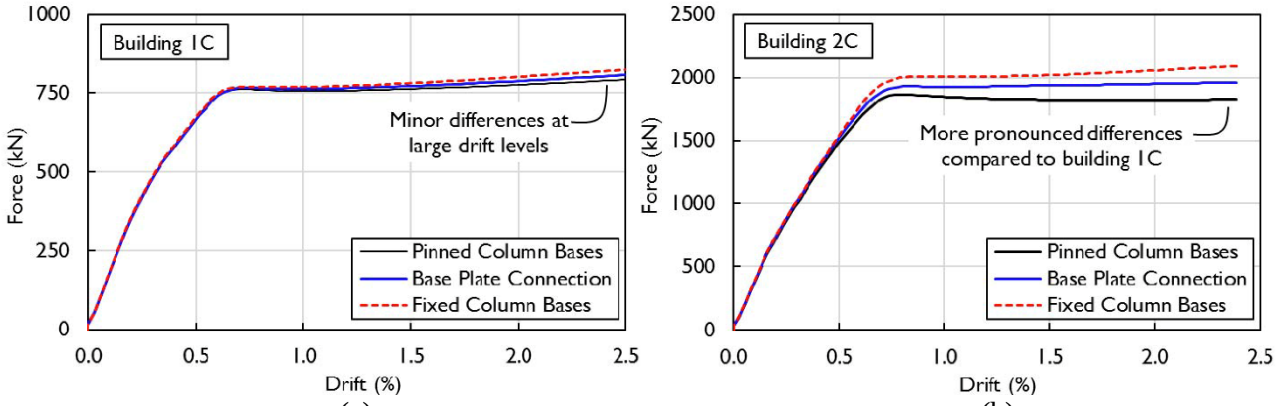

(a) (b)

Fig. 9 – Pushover analysis results: (a) building 1C; (b) building 2C

4.4 Numerical Results

4.4.1 Pushover Analysis

Prior to subjecting the building model to the set of earthquake ground motion records shown in Figure 8, nonlinear pushover analyses were conducted. Figure 9 shows the pushover analysis results for the two prototype buildings and the three different support conditions: (1) pinned column bases, (2) fixed column bases and (3) realistic base plate connection model. The results show that both structures have very similar initial stiffness despite the different column boundary conditions. In the post-yield range, the results show that the base plate connection provides additional post-yield strength and stiffness when compared with pinned column bases, but not greater than the post-yield strength and stiffness of an assumed fixed column boundary condition. Comparing the results from the two prototype buildings, the results show that the relative increase in post-yield strength and stiffness when considering the base plate connections in building 2C is greater, because there are more base plate connections. Overall, these results suggest that for ground motions that do not produce a maximum drift of more than 1%, the response of the structures will be similar. However, for large earthquakes and a large inelastic demand, the influence of the column base fixity may become more significant.

4.4.2 Nonlinear Time-history Analysis

Nonlinear time-history analyses were conducted to evaluate the influence of column base fixity on the inelastic seismic response of the two prototype buildings. Both buildings were subjected to the set of 15 ground motion records shown in Fig. 8. Figure 10 shows the maximum roof displacement response (drift in %) for each ground motion and each different column base support condition. Note that there were material nonlinearity convergence problems with one of the interface subduction earthquakes, and thus it was excluded from the analysis results in Fig. 10. Overall, the results demonstrate that although there is some variability in the maximum response of the two prototype buildings when different support conditions are considered, it does not have a large influence on the maximum displacement response of each structure. For both buildings, the maximum roof drift remains below 1.5% for all of the ground motion records, and as was anticipated from the pushover analysis results, no significant differences are observed in the seismic response of the buildings except for large structural demands (drifts over 2%).

Figure 11 shows the response of each prototype building for a select ground motion record. The results for building 1C subjected to a crustal earthquake show that the degree of column base fixity does not have a significant effect on the seismic response of the building. The maximum drift and displacement time-history over the course of the ground motion are very similar for all three support conditions. The force-deformation response of the braces and ductility demand are also very comparable. Alternatively, Figure 11b shows the response of building 2C under the effects of a subduction ground motion record. The results confirm that the peak roof displacements of the building with different degrees of column base fixity are very comparable. However, the results also show that following the large acceleration pulse at the beginning of the ground

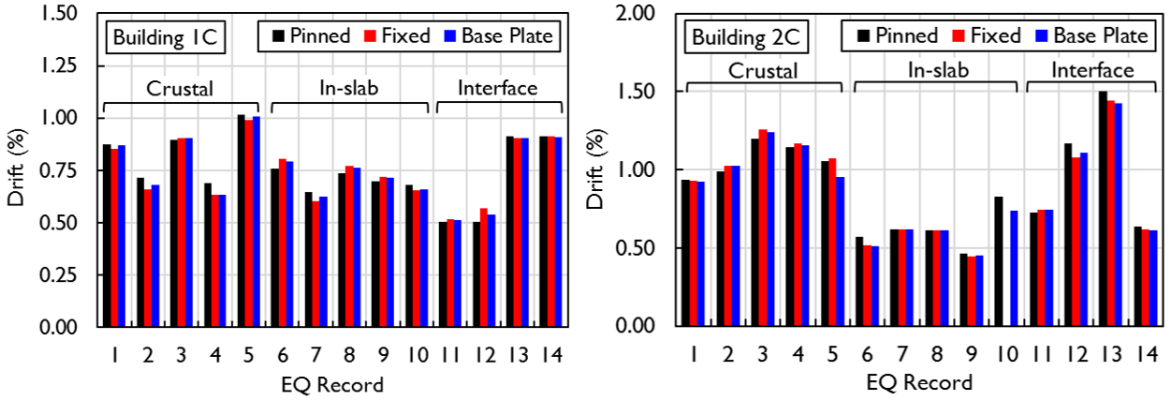

(a) (b)

Fig. 10 – Comparison of maximum displacement response: (a) building 1C; (b) building 2C

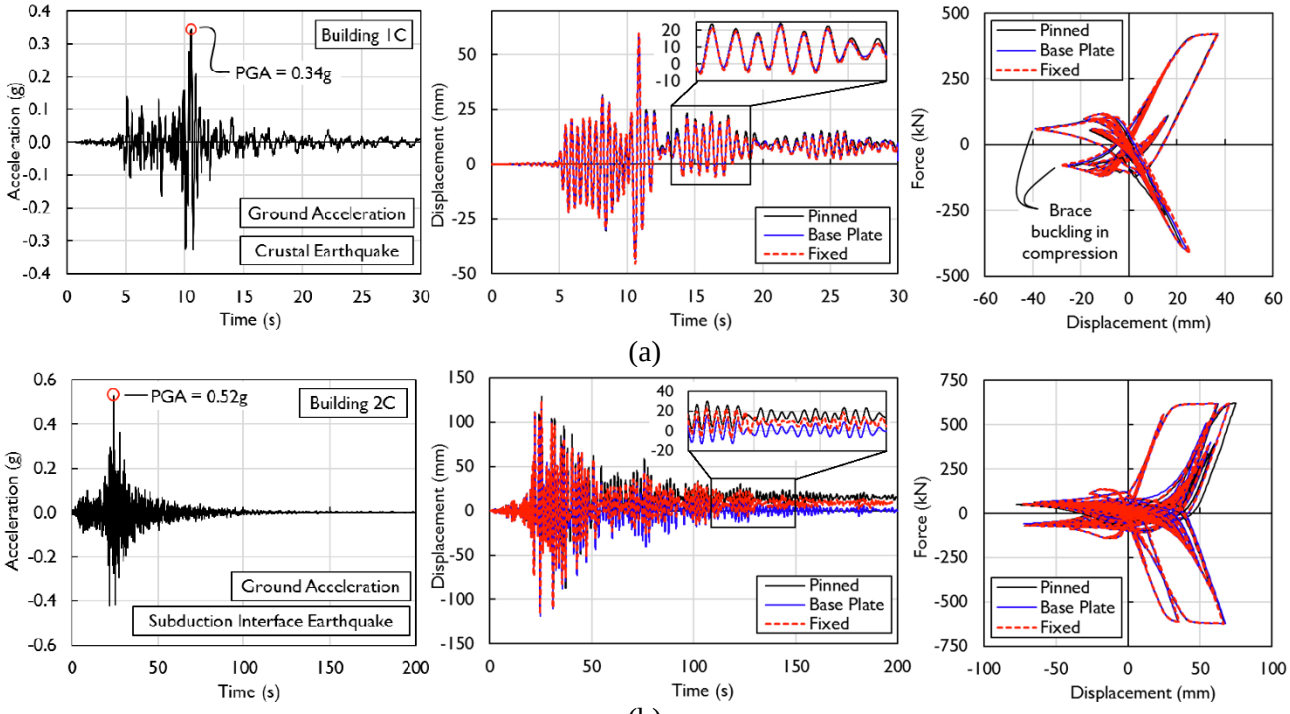

(a)

(b)

Fig. 11 – Nonlinear time history analyses results for two ground motions: (a) building 1C; (b) building 2C.

motion, the structure experiences a slightly different post-peak response depending on the support conditions. These results suggest that although the degree of column base fixity has little effect on the maximum displacement of the two buildings, it may influence other important structural response parameters, such as residual drift, particularly for long-duration subduction earthquakes.

5. Conclusions

This paper is a preliminary investigation into the effects of column base fixity on the global seismic response of single storey braced frames with flexible roof diaphragms. Experimental results and detailed three-dimensional modeling of exposed base plate connections in ABAQUS have demonstrated that base plate connections can exhibit some strength and stiffness and have the potential to influence a structures global seismic response. Based on these observations, a simple two-dimensional numerical model suitable for nonlinear time-history analysis was developed in OpenSees. The model is shown to be able to predict the

strength, stiffness, and self-centering cyclic behaviour of exposed base plate connections under cyclic load. Based on promising results from the simple model, it is implemented in the nonlinear time-history analysis of two single storey prototype steel concentrically braced frames with flexible roof diaphragms. A novel shell element modeling approach was shown to be effective in capturing the dynamic response of the flexible steel deck roof diaphragm. Pushover analysis results showed that modeling a realistic base plate connection did increase the post-yield stiffness and strength of the structures but their initial stiffness and strength at low levels of lateral drift (<1-1.5%) is not greatly affected by the degree of column base fixity. The nonlinear time-history analysis showed minor differences in structural response depending on the type of input ground motion, but the response in terms of maximum drift was not significantly different for varying degrees of column base fixity. The results did show that some differences in residual drift may be observed for long subduction-type ground motions, but warrants further investigation. Future work will focus on additional prototype buildings to better define the influence of column base fixity for a wider range of building design parameters.

6. Acknowledgements

The authors would like to acknowledge the postdoctoral fellowship provided by the Natural Science and Engineering Research Council of Canada (NSERC). Experimental data provided by Gomez et al. (2010) accessed through the DEEDS data centre hub to calibrate the numerical models is also gratefully acknowledged.

7. References

[1] DeWolf J, Sarisley E (1980): Column Base Plates with Axial Loads and Moments. *Journal of Structural Division* **106** (11): 2167-84.

[2] Picard A, Beaulieu D (1986): Rotational Restraint of a Simple Column Base Connection. *Canadian Journal of Civil Engineering.* 49-57.

[3] Burda J, Itani A (1999): Studies of seismic behaviour of steel base plates. *Report No. CCEER 99-7*, Center of Civil Engineering Earthquake Research, Department of Civil and Environmental Engineering, University of Nevada.

[4] Ermopoulos J, Stamatopoulos G (1996): Mathematical Modeling of Column Base Plate Connections. *Journal of Construction Steel Research*, 199679-100.

[5] Drake R, Elkin S (1999) Beam-column Base Plate Design–LRFD Method. *AISC Engineering Journal*, **36** (1): 29-38.

[6] Fisher J, Kloiber L (2006): Base Plate and Anchor Rod Design. *AISC Steel Design Guide One*, American Institute of Steel Construction, 2nd Edition, Chicago, IL.

[7] Gomez I, Kanvinde A, Deierlein G (2010): Exposed Column Base Connections Subjected to Axial Compression and Flexure. *Final Report* to the American Institute of Steel Construction (AISC).

[8] Kanvinde AM, Grilli D, Zareian F (2012): Rotational Stiffness of Exposed Column Base Connections – Experiments and Analytical Models. *Journal of Structural Engineering*, **138** (5), 549-60

[9] Kanvinde AM, Jordan SJ, Cooke RJ (2013): Exposed Column Base Plate Connections in Moment Frames – Simulations and Behavioural Insights. *Journal of Construction Steel Research*, **84**, 82-93.

[10] Krawinkler H, Gupta A, Medina R, Luco N (2000): Loading Histories for Seismic Performance Testing of SMRF Components and Assemblies. *SAC Joint Venture, Report No. SAC/BD-00/10*. Richmond, CA.

[11] ABAQUS (2016): ABAQUS User's Manual, *Version 6.13*.

[12] Popovics S (1973): A Numerical Approach to the Complete Stress-Strain Curves of Concrete. *Cement and Concrete Research*, **3** (5), 583-599.

[13] McKenna, F., Fenves, G. L. and Scott, M. H. (2000). "Open system for earthquake engineering simulation". University of California, Berkeley, California, USA.

[14] NRC (2015): National building code of Canada. Associate Committee on the NBC, NRC Council. Ottawa, Canada.

[15] CSA (2014): Design of Steel Structures. *CAN/CSA S16-14*. Toronto, Canada.

